Journal of Alloys and Compounds 522 (2012) 35–38

Contents lists available at SciVerse ScienceDirect

Journal of Alloys and Compounds

journal homepage: www.elsevier.com/locate/jallcom

Formation and structure of Cu–Zr–Al ternary metallic glasses investigated by ion beam mixing and calculation

X. Bai, J.H. Li, Y.Y. Cui, Y. Dai, N. Ding, B.X. Liu*

Advanced Materials Laboratory, Department of Materials Science and Engineering, Tsinghua University, Beijing 100084, China

ARTICLE INFO

Article history:
Received 9 October 2011
Received in revised form 10 January 2012
Accepted 10 January 2012
Available online 28 January 2012

Keywords:
Cu–Zr–Al system
Ion beam mixing
Amorphous phase
Structure factor

ABSTRACT

The $Cu_{12.6}Zr_{40.5}Al_{46.9}$ and $Cu_{32.7}Zr_{6.7}Al_{60.6}$ amorphous alloys are synthesized in metallic multilayered films by ion beam mixing in the present study. Formation mechanism of amorphous phases is discussed in terms of the atomic collision theory. To further analyze the structure and composition of the obtained Cu–Zr–Al metallic glasses, structure factor $S(q)$ is calculated based on the results of molecular dynamics simulations. It is found that the $Cu_{12.6}Zr_{40.5}Al_{46.9}$ and $Cu_{32.7}Zr_{6.7}Al_{60.6}$ metallic glasses are mainly consisted of Al–Zr and Al–Al, Cu–Cu amorphous phases, respectively. The calculated results turn out to match well with the experimental observation.

1. Introduction

Since the first finding of millimeter–diameter glassy rods in the Pd–Cu–Si system [1], the bulk metallic glasses (BMGs) have attracted tremendous attention due to their superior mechanical properties and excellent corrosion resistance [2–5]. In particular, there has been a huge interest in the Cu–Zr–Al system currently, which is expected to be an advantaged candidate for BMGs because of its high glass-forming ability (GFA) [6,7]. A series of Cu–Zr–Al based BMGs or BMG composites have also been obtained in experiments. The obtained BMGs exhibit extraordinarily high strength and good compressive ductility [8–11]. To clarify the atomic structures and compositions of the Cu–Zr–Al BMGs, investigations have been conducted from both experimental and theoretical aspect, such as using molecular dynamics (MD) simulations by Wang et al. [12] and in situ synchrotron X-ray scattering measurements by Fan et al. [13].

To study the glass-forming-ability or glass-forming-region of the Cu–Zr–Al system, the long range smoothed second-moment-approximation of tight-binding potential for the Cu–Zr–Al system has been constructed by fitting the physical properties of Cu, Zr, Al and their compounds [14]. Based on the constructed potential, MD simulations were carried out using solid solution model to compare the relative stability of the crystalline solid solution versus its disordered counterpart as a function of solute concentration. Simulations reveal that the physical origin of metallic glass formation is crystalline lattice collapsing while solute concentration exceeding critical value, thus predicting a hexagonal composition region, within which the Cu–Zr–Al ternary metallic glass formation is energetically favored, as shown in Fig. 1 [14].

For the experimentally obtained Cu–Zr–Al metallic glasses, the great majority of their compositions fall within the predicted glass-forming favored region. Further inspecting Fig. 1, one may find that the experimental work has so far been focused on the Cu–Zr-based system with minor addition of Al [15–17]. In the present study, two Cu–Zr–Al multilayered films were designed with the overall compositions of $Cu_{12}Zr_{40}Al_{47}$ and $Cu_{32}Zr_6Al_{62}$, which are exactly in the predicted hexagonal region. On one hand, we can study the metallic glass formation in Al-rich composition, because whether the Cu–Zr–Al metallic glasses can be obtained in the Al–Zr-based or the Al–Cu-based system by experiment is still an open issue. On the other hand, the experimental results can also serve as a comparison with the MD simulations.

2. Cu–Zr–Al ternary metallic glasses formed by ion beam mixing

Considering the individual and total thickness of Cu–Zr–Al multilayered films, the samples were both designed to be 8 layers. Two sets of initial multilayered films were prepared by depositing alternatively pure Cu (99.99%), Zr (99.99%) and Al (99.99%) at a rate of 0.2 Å/s onto NaCl single crystal substrates in an e-gun evaporation system with a vacuum level on the order of 10^{-7} Pa. The as-deposited Cu–Zr–Al multilayered films were then irradiated by 200 keV xenon ions in an implanter with a vacuum level better than 5×10^{-4} Pa and the irradiation dose was in a range from

* Corresponding author. Tel.: +86 10 6277 2557; fax: +86 10 6277 1160.
E-mail address: dmslbx@tsinghua.edu.cn (B.X. Liu).

0925-8388/$ – see front matter © 2012 Elsevier B.V. All rights reserved.
doi:10.1016/j.jallcom.2012.01.060

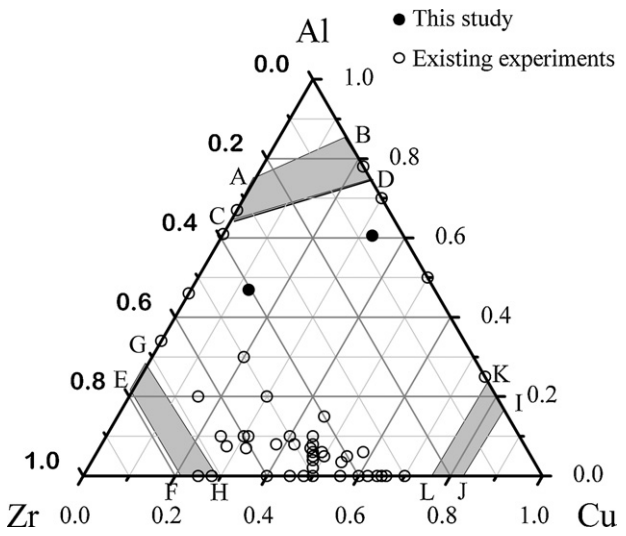

Fig. 1. The crystal-amorphous state phase diagram derived from MD simulations for the Cu–Zr–Al ternary system [11], and the "blank" region delimited by the contour line CDKLHG predicts the formation of amorphous phase.

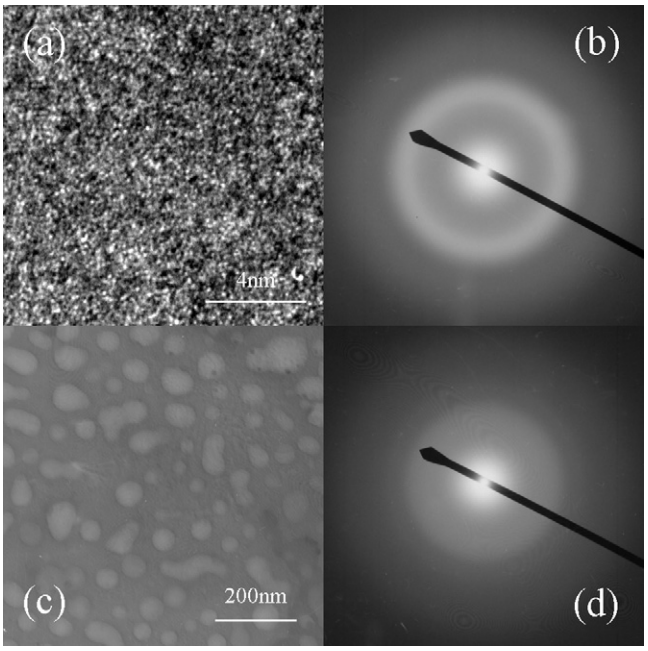

Fig. 2. HRTEM image (a) with the corresponding SAD pattern (b) of the $Cu_{12.6}Zr_{40.5}Al_{46.9}$ alloy and bright field image (c) with the corresponding SAD pattern (d) of the $Cu_{32.7}Zr_{6.7}Al_{60.6}$ alloy after an irradiation dose of 3×10^{15} Xe^+/cm^2.

8×10^{14} to 5×10^{15} Xe^+/cm^2. During irradiation, the sample holder was always cooled by liquid nitrogen (77 K) and the ion current density was confined to be about 2 $\mu A\,cm^{-2}$ to avoid overheating effect. The as-deposited and irradiated Cu–Zr–Al samples were examined by transmission electron microscopy (TEM) and high resolution transmission electron microscopy (HRTEM) for structural characterization. X-ray fluorescence (XRF) was used to determine the compositions of the samples.

The composition of the two sets of as-deposited samples are determined by XRF to be $Cu_{12.6}Zr_{40.5}Al_{46.9}$ and $Cu_{32.7}Zr_{6.7}Al_{60.6}$, which are exactly located in the amorphous formation region predicted by MD simulation [14]. Metallic glasses were obtained in the $Cu_{12.6}Zr_{40.5}Al_{46.9}$ and $Cu_{32.7}Zr_{6.7}Al_{60.6}$ samples upon ion beam mixing (IBM) in irradiation dose ranges of 3×10^{15} to 5×10^{15} and 1×10^{15} to 5×10^{15} Xe^+/cm^2, respectively. The HRTEM graphic and the selected area diffraction (SAD) pattern of the irradiated $Cu_{12.6}Zr_{40.5}Al_{46}$ sample are shown in Fig. 2(a) and (b), respectively. From Fig. 2(a) and (b), it can be seen that a unique amorphous phase was synthesized in the $Cu_{12.6}Zr_{40.5}Al_{46}$ samples. Fig. 2(a) presents the micro-morphology of an homogeneous metallic glass, and Fig. 2(b) shows the halo due to the amorphous structure. In the cases of the $Cu_{32.7}Zr_{6.7}Al_{60.6}$ irradiated sample, the bright field image and selected area diffraction (SAD) pattern are shown in Fig. 2(c) and (d), respectively. Fig. 2(c) shows the bright field image with a contrast that can be explained by the presence of an amorphous dual-phase resulting from a phase separation. The SAD pattern of Fig. 2(d) shows a unique broad halo as a consequence of the overlapped halos of the two amorphous phases, indicating a quite similar structure of the two metallic glasses. For further analysis, energy-dispersive spectrum (EDS) was utilized to determine the composition of the separated phases formed in the $Cu_{32.7}Zr_{6.7}Al_{60.6}$ samples, however, the composition differences could not be detected possibly due to the limitation of instrument accuracy.

By comparing the halos shown in Fig. 2(b) and (d), it can be found that their locations are varied, showing that there are some structural or compositional differences existing between the two amorphous phases. Based on the camera constant and measured radius of halos in SAD patterns, the average distances of nearest-neighbor atoms were estimated to be 2.30 Å and 2.76 Å for the $Cu_{12.6}Zr_{40.5}Al_{46.9}$ and $Cu_{32.7}Zr_{6.7}Al_{60.6}$ metallic glasses, respectively. The structures and compositions of the two metallic glasses will be discussed in detailed in Section 3.

According to the atomic collision theory [18,19], the process of IBM in the Cu–Zr–Al multilayered films occurs as follows: initially, a sequence of ballistic collisions induce the interfacial mixing in the Cu–Zr–Al multilayered films upon ion irradiation, and after irradiation to an adequate dose, atomic mixing would result in forming a highly energetic and disordered Cu–Zr–Al atomic mixture. When the atomic collision cascade is eventually terminated, the highly energetic mixture has to relax toward equilibrium. However, the relaxation period is extremely short, lasting for about 10^{-10} s, so only a very minor atomic rearrangement could take place. Thus, the complete relaxation of the highly energetic state may become frustrated, and therefore the disordered state was preserved, leading to the formation of amorphous phases in the $Cu_{12.6}Zr_{40.5}Al_{46.9}$ and $Cu_{32.7}Zr_{6.7}Al_{60.6}$ samples.

3. Structural quantities of the Cu–Zr–Al metallic glasses

As shown above, the Cu–Zr–Al amorphous alloys were obtained by IBM in the $Cu_{12.6}Zr_{40.5}Al_{46.9}$ and $Cu_{32.7}Zr_{6.7}Al_{60.6}$ samples, and the compositions were right in the predicted glass-forming favored region by MD simulations. Interestingly, some structural or compositional differences were also found in the two amorphous phases synthesized by IBM. To develop a better understanding of the atom configurations in the amorphous alloys, structure factor $S(q)$ [20,21] as a function of wave vector q, was derived for the two Cu–Zr–Al alloys.

From the atom positions obtained in MD simulations, the structure factor $S(q)$ can be calculated as following. Specifically, in a cubic box, we may examine fluctuations for which $k = (2\pi/L)(k_x, k_y, k_z)$, where L is the box length and k_x, k_y and k_z are integers. One quantity of interest is the spatial Fourier transform of the number density [22]

$$\rho(k) = \sum_{i=1}^{N} \exp(i\vec{k} \cdot \vec{r}_i) \quad (1)$$

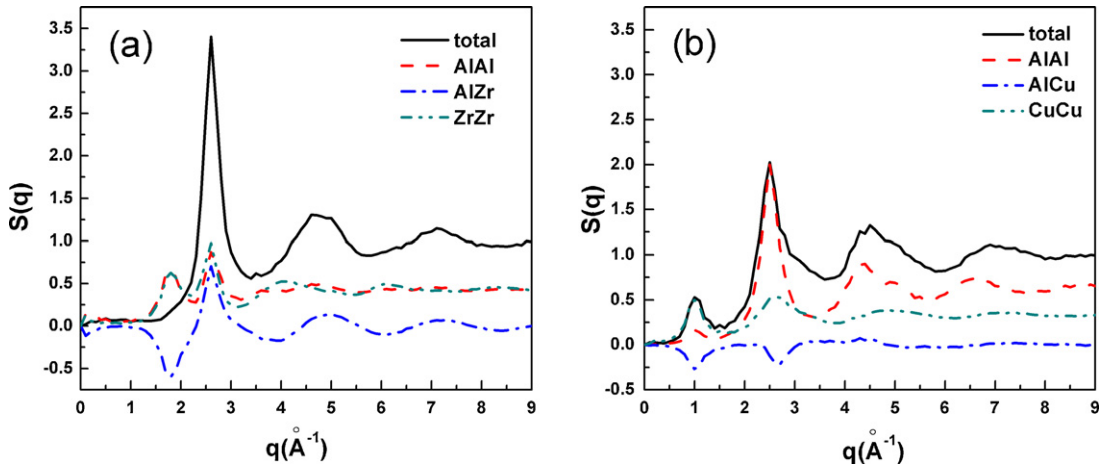

Fig. 3. Calculated total and partial static structure factors of the $Cu_{12.6}Zr_{40.5}Al_{46.9}$ (a) and $Cu_{32.7}Zr_{6.7}Al_{60.6}$ (b) samples.

Fluctuations in $\rho(k)$ are related to the structure factor $S(q)$

$$S(q) = N^{-1}\langle\rho(q)\rho(-q)\rangle \quad (2)$$

which may be measured by neutron or X-ray scattering experiments. Thus, $S(q)$ describes the Fourier components of density fluctuations in the samples. It is related, through a three-dimensional Fourier transform to the pair distribution function, and $S(q)$ can be expressed in terms of partial structure factors as

$$S(q)\frac{\sum\sqrt{c_i c_i}f_i f_j S_{ij}(q)}{\sum c_i f_i^2} \quad (3)$$

where $S_{ij}(q)$ are Ashcroft–Langreth's [23] partial structure factors

$$S_{ij}(q) = \delta_{ij} + \sqrt{c_i c_j}\rho\int_0^\infty [g_{ij}(r) - 1]\frac{\sin(qr)}{qr}4\pi r^2\ dr \quad (4)$$

where ρ is the total number density, C_i is the concentration of the i species, and $f_i(q)$ are the X-ray scattering factors of the atoms of type i tabulated by Doly and Turner [24].

Based on the above formulas and MD simulation data in reference [14], the total and partial structure factors $S(q)$s of the $Cu_{12.6}Zr_{40.5}Al_{46.9}$ and $Cu_{32.7}Zr_{6.7}Al_{60.6}$ samples were calculated, and the results are shown in Fig. 3(a) and (b), respectively. In the figures, both total $S(q)$ curves are mainly consisted of first sharp peak and second, third low-lying peaks, and when q increases up to 10 Å^{-1}, the curves begin converging to 1. It can be observed that the two total $S(q)$ curves both correspond to amorphous phases, and the first sharp peaks present nearest-neighbor atoms. For comparison, the two total $S(q)$ curves are both presented in Fig. 4, and the first sharp peaks locate at $q = 2.75$ and $q = 2.50$ Å^{-1}, for the $Cu_{12.6}Zr_{40.5}Al_{46.9}$ and $Cu_{32.7}Zr_{6.7}Al_{60.6}$ samples, respectively. It is therefore determined that the average distances of nearest-neighbor atoms are calculated to be 2.29 Å and 2.51 Å. As mentioned in the IBM experimental results, the halo locations of the two metallic glasses are different, by comparing the two sets of nearest-neighbor atom distances, we found a good agreement between the calculated and the IBM experimental results.

From Fig. 3(a), it is found that the total $S(q)$ of $Cu_{12.6}Zr_{40.5}Al_{46.9}$ samples is mainly consisted of Al–Al, Al–Zr and Zr–Zr partial $S(q)$s, as the contributions of other curves such as Al–Zr, Cu–Zr and Cu–Cu are nearly zero, they have thus not been shown in the figure. Accordingly, it could be supposed that the metallic glass obtained in the $Cu_{12.6}Zr_{40.5}Al_{46.9}$ samples is consisted of Al–Zr based unique amorphous phases with some few Cu atoms dissolved in it. Basically, the deduction is considered to be reasonable because of the following actual factors: the atomic percent of Cu in $Cu_{12.6}Zr_{40.5}Al_{46.9}$ samples is at around 12%, and also, Cu atoms could easily be dissolved into the Al–Zr-based matrix because of the minor atomic radius. Similar calculated results are observed in Fig. 3(b), and the amorphous matrix in the $Cu_{32.7}Zr_{6.7}Al_{60.6}$ samples is reflected by the total $S(q)$ curve. In Fig. 3(b), Al–Al, Al–Cu and Cu–Cu partial $S(q)$ curves are listed, and Al–Zr, Cu–Zr and Zr–Zr partial $S(q)$s are neglected since their contributions are small. Accordingly, it is found that the contribution of Al–Al partial $S(q)$ is dominant, followed by that Cu–Cu partial one, and the contribution of cross-term Cu–Al partial $S(q)$ is nearly zero, which is different from the results of $Cu_{12.6}Zr_{40.5}Al_{46.9}$ samples. Based on the calculated results, the metallic glasses synthesized in the $Cu_{32.7}Zr_{6.7}Al_{60.6}$ samples are mainly consisted of Al–Al and Cu–Cu amorphous phases, consisting with the results of phase separation of two amorphous phases in IBM experiment. Therefore, we can conclude that Al–Al and Cu–Cu based metallic glasses were both synthesized in the whole $Cu_{32.7}Zr_{6.7}Al_{60.6}$ irradiated samples, and only trace amount of Al–Cu combination were existed.

Based on the discussion above, the $Cu_{12.6}Zr_{40.5}Al_{46.9}$ and $Cu_{32.7}Zr_{6.7}Al_{60.6}$ irradiated samples are mainly consisted of Al–Zr, and Al–Al, Cu–Cu based amorphous phases, respectively. According to Miedema's model [25], the formation heats of Al–Zr and Al–Cu are −83 and −10 kJ/mol, respectively, indicating that there is a more intense binding force between Al and Zr rather than Al and Cu, which makes the combination of atoms Al and Zr closer, i.e. a

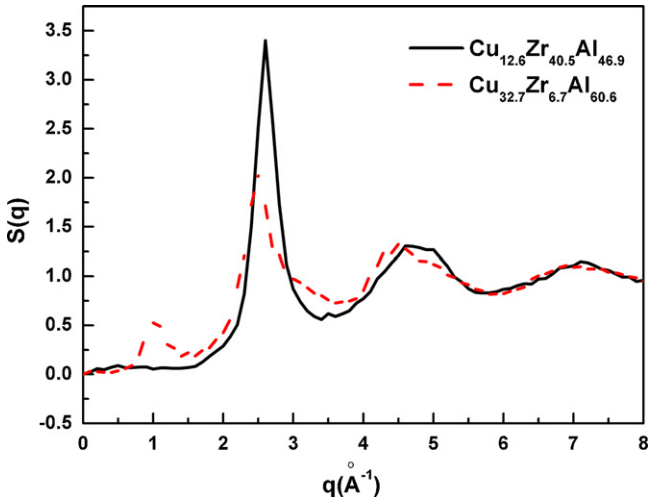

Fig. 4. Calculated total static structure factors of the $Cu_{12.6}Zr_{40.5}Al_{46.9}$ and $Cu_{32.7}Zr_{6.7}Al_{60.6}$ samples.

shorter distance of nearest-neighbor atoms. Otherwise, the formation heat of Al–Cu is near to zero, which is not effective enough for driving the combination of Al and Cu atoms, and it is this reason that a phase separation occurred in the $Cu_{32.7}Zr_{6.7}Al_{60.6}$ samples instead of forming unique Al–Cu based amorphous phases.

4. Conclusions

In summary, for the Cu–Zr–Al system, $Cu_{12.6}Zr_{40.5}Al_{46.9}$ and $Cu_{32.7}Zr_{6.7}Al_{60.6}$ metallic glasses were obtained by ion beam mixing, and the composition locates exactly in the Cu–Zr–Al glass-forming favored region calculated by MD simulations. According to the MD simulation results, structure factors of the two Cu–Zr–Al alloys were calculated and the results revealed that the $Cu_{12.6}Zr_{40.5}Al_{46.9}$ and $Cu_{32.7}Zr_{6.7}Al_{60.6}$ metallic glasses are mainly consisted of Al–Zr and Al–Al, Al–Cu based amorphous phases, respectively, showing a quite good agreement with the available experimental results.

Acknowledgments

The authors are grateful for the financial support from the National Natural Science Foundation of China (50971072, 51131003), the Ministry of Science and Technology of China (2011CB606301), and the Administration of Tsinghua University.

References

[1] H.S. Chen, Acta Metall. 22 (1974) 1505–1511.
[2] J. Schroers, Adv. Mater. 22 (2010) 1566–1597.
[3] A. Inoue, Acta Mater. 48 (2000) 279–306.
[4] W.H. Wang, C. Dong, C.H. Shek, Mater. Sci. Eng. R 44 (2004) 45–89.
[5] A.L. Greer, Mater. Today 12 (2009) 14–22.
[6] G.V. Afonin, S.V. Khonik, R.A. Konchakov, Yu.P. Mitrofanov, N.P. Kobelev, K.M. Podurets, A.N. Tsyplakov, L.D. Kaverin, V.A. Khonik, Intermetallics 19 (2011) 1298–1305.
[7] J. Antonowicz, A. Pietnoczka, W. Zalewski, R. Bacewicz, M. Stoica, K. Georgarakis, A.R. Yavari, J. Alloys Compd. 509S (2011) S34–S37.
[8] Y. Wu, H. Wang, H.H. Wu, Z.Y. Zhang, X.D. Hui, G.L. Chen, D. Ma, X.L. Wang, Z.P. Lu, Acta Mater. 59 (2011) 2928–2936.
[9] A. Castellero, T.A. Baser, J. Das, P. Matteis, J. Eckert, L. Battezzati, M. Baricco, J. Alloys Compd. 509S (2011) S99–S104.
[10] X.D. Wang, Q.K. Jiang, Q.P. Cao, J. Bednarcik, H. Franz, J.Z. Jiang, J. Appl. Phys. 104 (2008) 093519 1–093519 5.
[11] T.L. Cheung, C.H. Shek, J. Alloys Compd. 434 (2007) 71–74.
[12] Y. Wu, H. Wang, H.H. Wu, Z.Y. Zhang, X.D. Hui, G.L. Chen, D. Ma, X.L. Wang, Z.P. Lu, J. Alloys Compd. 59 (2011) 2928–2936.
[13] C. Fan, Y. Ren, T. Liu, P.K. Liaw, H.G. Yan, T. Egami, Phys. Rev. B 83 (2011) 195207 1–195207 6.
[14] Y.Y. Cui, T.L. Wang, J.H. Li, Y. Dai, B.X. Liu, Phys. Chem. Chem. Phys. 13 (2011) 4103–4108.
[15] D. Wang, H. Tan, Y. Li, Acta Mater. 53 (2005) 2969–2979.
[16] K. Georgarakis, A.R. Yavari, D.V. Louzguine-Luzgin, J. Antonowicz, Appl. Phys. Lett. 94 (2009) 191912 1–191912 3.
[17] Y.Q. Cheng, E. Ma, H.W. Sheng, Phys. Rev. Lett. 102 (2009) 245501 1–245501 4.
[18] M.W. Thompson, Defects and Radiation Damage in Metals, Cambridge University Publishing, Cambridge, 1969.
[19] B.X. Liu, W.S. Lai, Q. Zhang, Mater. Sci. Eng. R 29 (2000) 1–48.
[20] S. Dalgic, M. Colakogullari, J. Non-Cryst. Solids 353 (2007) 1936–1940.
[21] G. Kahl, Phys. Rev. A 43 (1991) 822–834.
[22] M.P. Allen, D.J. Tildesley, Computer Simulation of Liquids, Oxford Science Publishing, Clarendon, 1981.
[23] N.W. Ashcroft, D.C. Langreth, Phys. Rev. 156 (1967) 685–692.
[24] P.A. Doyle, P.S. Turner, Acta Crystallogr. A 24 (1968) 390–397.
[25] F.R. De Boer, R. Boom, W.C.M. Matterns, A.R. Miedema, A.K. Niessen, Cohesion in Metals: Transition Metal Alloys, North-Holland Publishing, Amsterdam, 1988.